FORMIN-2 IN ESTABLISHING THE SPINAL NEURONAL CIRCUITRY

B.S - M.S THESIS

AJESH JACOB

20101040

UNDER GUIDANCE OF

DR. AURNAB GHOSE

BIOLOGY DEPARTMENT, IISER PUNE

Certificate

This is to certify that this dissertation entitled “Formin-2 in establishing the spinal neuronal circuitry” towards the partial fulfilment of the BS-MS dual degree programme at the Indian Institute of Science Education and Research (IISER), Pune represents original research carried out by Ajesh Jacob at IISER Pune under the supervision of Dr. Aurnab Ghose, Assistant Professor, Biology Division, IISER Pune during the academic year 2014 - 2015.

Date: 25 March, 2015

Dr. Aurnab Ghose
Assistant Professor
IISER Pune

Declaration

I hereby declare that the matter embodied in the report "Formin-2 in establishing the spinal neuronal circuitry" are the results of the investigations carried out by me at the Department of Biology, IISER Pune, under the supervision of Dr. Aurnab Ghose and the same has not been submitted elsewhere for any other degree.

Ajesh Jacob
20101040
B.S – M.S Student
IISER Pune

ABSTRACT

The proper functioning of a mature nervous system depends on the complex neuronal circuits. One of the critical phases of neuronal development is the formation of specific connections between the neurons and their target. The growth cone at the distal tip helps the axon to navigate through a pool of guidance cues. Growth cone contain a large amount of dynamic cytoskeletal elements and its motility is dependent on the polymerization of actin. Several factors control the dynamics of actin polymerization. Actin nucleators can increase the rate of addition of G-monomers to the actin filament and can nucleate the formation of a new filament. Actin nucleators are also required for cue mediated directional motility. Studies in our lab has shown the presence of the actin nucleators such as Fmn2 and Spire2, in the developing spinal cord. Cultured neurons showed decreased filopodia number and length and unstable focal adhesions, when the Fmn2 was depleted. This project primarily studied the role of Fmn2 in dI1 commissural neurons. Fmn2 depleted dI1 commissural neurons showed midline crossing defects. When mFmn2 was expressed specifically in the dI1 neurons, in the background of gFmn2 knockdown, the dI1 axons crossed the midline similar to the wild type. The rescue by mFmn2 underscores the evolutional conserved nature of Fmn2 function in the dI1 neurons as the mouse ortholog is able to rescue axon guidance of these neurons in the chick spinal cord. Expression of gFmn2 N terminal fragment also caused midline crossing defects in dI1 commissural neurons.

Table of contents

List of figures

Acknowledgements

I take this opportunity to thank my mentor Dr. Aurnab Ghose for his valuable, inspiring and encouraging guidance and for providing me with scientific freedom that enabled me to work enthusiastically and molded my scientific development.

I would like to thank Dr. L S Shashidhara for his valuable inputs and my lab members Abhishek, Ketakee, Tanushree, Sampada, and all others for assisting, teaching and encouraging me all through the project. I thank my friends and family for showing faith and providing confidence during my entire IISER life.

Chapter 1

INTRODUCTION

1) Axonal guidance by Growth Cone

The proper functioning of a mature nervous system depends on the complex neuronal circuits. One of the critical phases of neuronal development is the formation of specific connections between the neurons and their target. For establishing the connections sometimes the axons has to move a long distance from its origin. For example, the dI1 and dI2 commissural neurons in the spinal cord project their axons to the regions in the hindbrain, cerebellum and isthumus (Sakai et al., 2012).

The axons have a specialized structure at the distal tip known as 'Growth Cone', which helps them to navigate through a pool of guidance cues. The cues can be short range or long range and attractive or repulsive. Short range guidance cues are primarily cell adhesion molecules such as FasII, NrCAM, Sema and Slit (Lowery and Van Vactor, 2009). Long range cues are primarily diffusible molecules such as Netrin, Wnt, Shh and BMP, originating from a distance source (Lowery and Van Vactor, 2009). Growth cones exhibit a positive chemotaxis to an attractive cue and grow towards it. Whereas it collapse or turn away and grow in a different direction when it experience a repulsive guidance cue.

Growth cone is comprised of dynamic cytoskeletal elements. Based on the cytoskeletal distribution the growth cone can be separated into three domains – peripheral (P) domain, transition (T) domain and central (C) domain (Lowery and Van Vactor, 2009) (Fig 1). The P domain encloses the mesh-like branched actin network, which form the lamellipodia and long bundled actin filaments, which give rise to filopodia. Some exploratory microtubules are also present in this domain. The C domain contains the stable microtubule bundles from the axonal shaft, along with numerous

organelles, vesicles and central actin bundles. The T domain is the interface between the P and C-domains, where the actomyosin contractile structures are present.

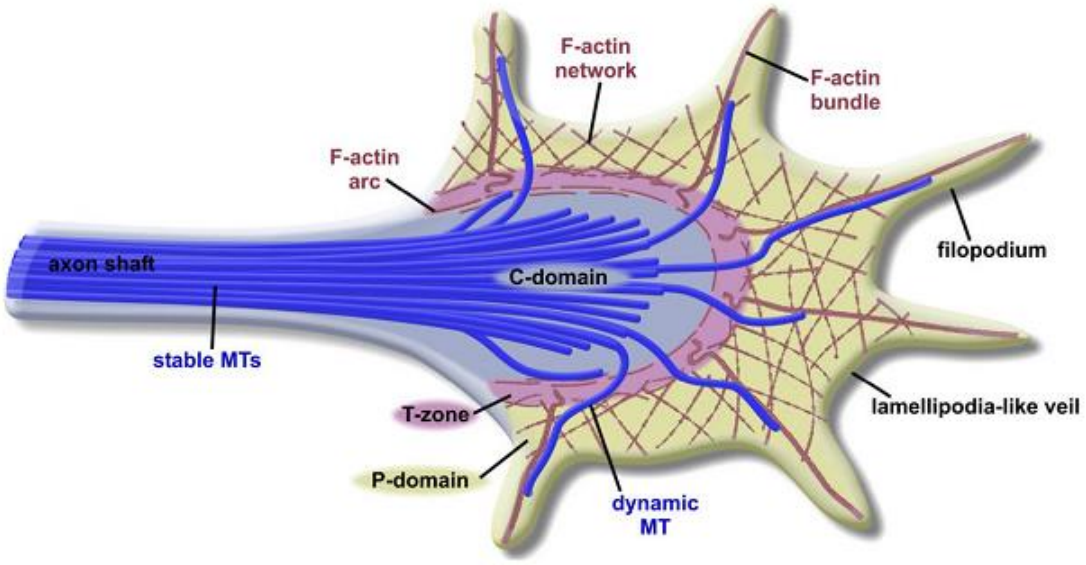

Fig 1: Growth cone structure. Schematic showing the domains in a growth cone along with the cytoskeletal elements. Adapted by permission from Macmillan Publishers Ltd: Nature Reviews Molecular Cell Biology (Lowery and Van Vactor, 2009), copyright 2009.

The shape of the growth cone and its motility is controlled by the dynamics of cytoskeletal elements. F-actin treadmilling and F-actin retrograde flow primarily controls the movement of a growth cone. Treadmilling includes the F-actin polymerization at the leading edge, F-actin severing at T domain and recycling of the G-actin back to leading edge (Lowery and Van Vactor, 2009). Retrograde flow is the backward movement of F-actin towards the T-domain caused by myosin-II driven actin transport and the pushing force exerted by the actin on the peripheral membrane as it polymerizes (Lowery and Van Vactor, 2009). The growth cone protrudes only if the polymerization rate is higher than the velocity of the retrograde flow. The membrane remains stationary when the polymerization rate and the retrograde flow balances. When a growth cone experience an adhesion substrate or an attractive cue, the coupling between actin cytoskeleton and

transmembrane adhesion receptors increases (Dent et al., 2011; Lowery and Van Vactor, 2009). This anchoring decreases the retrograde flow and promotes the actin polymerization to extend the leading edge. The C-domain microtubules then invade into the T-domain with the help of actomyosin contractile structure. These processes lead to the protrusion of growth cone.

2) Actin nucleators

Growth cone is dynamic in nature and its motility depends upon the polymerization of actin filaments. Several factors influence the rate of polymerization of actin. One such factor is the actin nucleators. Studies has shown that actin nucleators like Arp2/3 and Fmn2 are required for filopodia and lamellipodia formation in growth cone (Beeraka, 2014; Sahasrabudhe, 2015)(Korobova and Svitkina, 2008; San Miguel-Ruiz and Letourneau, 2014). Bead pulling assays and induction assays show the crucial role of actin nucleators in directed motility (Beeraka, 2014). Actin nucleators function by forming an actin-seed and increase the rate of F-actin formation from the G-actin monomers. Arp2/3, FH2 domain-containing proteins and WH2 domain-containing proteins are the three major classes of actin nucleators (Campellone and Welch, 2010).

Arp2/3 is a 220kDa complex comprising of Arpc1-Arpc5, Arp2 and Arp3 (Campellone and Welch, 2010). Arp2/3 is unique in its ability to both nucleate and mediate the branching of actin filaments. Arp2/3 functions by binding to the side of an existing actin filament and initiating the assembly of a new filament at an angle of 70^0 (Campellone and Welch, 2010). WH2 domain-containing nucleators include Spire, cordon-bleu, leiomodin families and several bacterial nucleators (Campellone and Welch, 2010). These proteins have a tandem cluster of three or more G-actin binding motifs including their characteristic WH2 domain (Campellone and Welch, 2010). The mode of action of the WH2 domain proteins are not clearly known. Evidences suggest that Spire cooperate with formins in actin nucleation and polymerization (Vizcarra et al., 2011).

Formins have the conserved formin homology (FH) domains, FH1 and FH2 (Higgs, 2005). Around 15 mammalian formins have been identified till now (Campellone and Welch, 2010). Based on the FH2 sequence divergence, they are categorized into seven different subclasses: Diaphanous (DIA), formin-related proteins in leukocytes (FRLs), Dishevelled-associated activators of morphogenesis (DAAMs), formin homology domain proteins (FHODs), formins (FMNs), delphilin and inverted formins (INFs) (Campellone and Welch, 2010; Higgs, 2005)

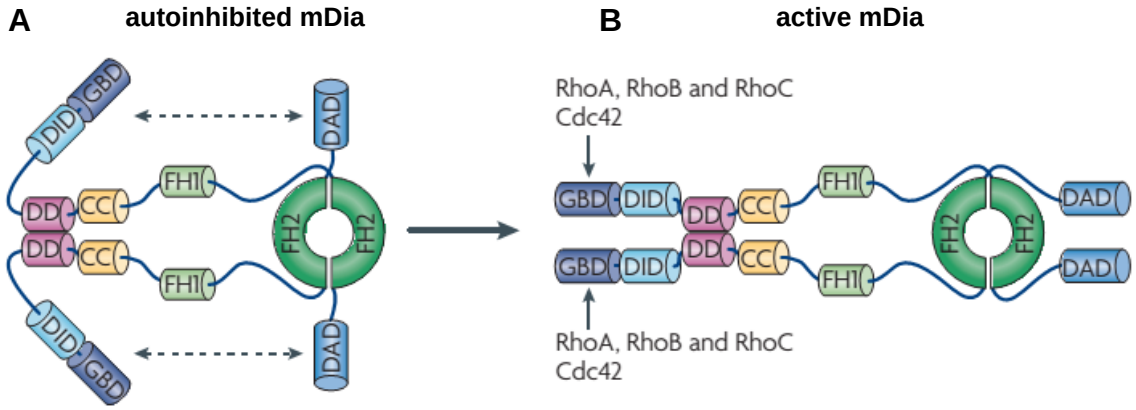

Fig 2. mDia activation by RhoGTPases. A) mDia autoinhibited by DID-DAD interaction B) RhoGTPases unleashes the mDia from autoinhibition. Adapted by permission from Macmillan Publishers Ltd: Nature Reviews Molecular Cell Biology (Campellone and Welch, 2010), copyright 2010.

Formins have a FH2 domain at the C-terminus that can bind to actin monomers. Studies show that FH2 domain is sufficient to trigger the actin nucleation (Pruyne et al., 2002; Pring et al., 2003). FH1 domain, N-terminus to the FH2 bind to the proflin-actin complex and promote the actin polymerization by increasing the local actin concentration (Campellone and Welch, 2010). Formins like mDia have a DAD domain at the C-terminus and a DID domain at the N-terminus (Li and Higgs, 2003). They are autoinhibited by the DID-DAD interaction and binding of a GTPase is required to unleash them from auto-inhibition(Li and Higgs, 2003; Campellone and Welch, 2010; Chesarone et al., 2010)(Fig 2) . They have a GTPase binding domain (GBD)

overlapping with the DID (Li and Higgs, 2003). In Formins including Fmn2, DID like and DAD like domains are not identified yet. Whether the Fmn2 activation is RhoGTPase dependent or not is also unknown.

In its active state Formins function as a homodimer. Crystallography and biochemical studies suggest that the homdimerizing creates a FH2 ring and this ring formation is crucial for the actin polymerization (Xu et al., 2004; Lu et al., 2007). A model for formin-mediated actin propose that the FH2 dimer associates with the barbed end of an actin filament and the FH1 domain recruits profiling-actin (Campellone and Welch, 2010).

Studies in our lab has shown an enrichment of Fmn2 and Spire2 in the developing chick spinal cord (K. Ghate, unpublished data). Some papers also report the expression of formins and Spire2 in the chick and mouse spinal cord (Schumacher et al., 2004). Developing spinal cord has a large number of migrating axons and these proteins may have some role in the axonal elongation and motility. However very few studies have been done which characterizes the actin nucleators in growth cones. Study in our lab has shown that inhibiting the Arp2/3 results in depletion of lamellipodia and the loss of directional motility in cultured DRGs (dorsal root ganglia) (Beeraka, 2014). Studies on cultured cerebellar granule neurons suggests the mDia involvement in axonal elongation (Arakawa et al., 2003). There has been no *in vivo* studies that characterize the actin nucleators in the developing neurons. Studies in our lab shows that Fmn2 is expressed in the spinal neurons and knock down of Fmn2 cause decrease in filopodia length and number and unstable focal adhesions (Sahasrabudhe, 2015).

3) Commissural neurons

Axonin-1 staining of Fmn2 knockdown spinals suggests Fmn2 is required for the development of commissural neurons in the spinal cord (Sahasrabudhe, 2015). Axonin-1 is a cell adhesion molecule expressed only in the commissural neurons (Stoeckli and Landmesser, 1995). In the wild type embryos commissural neurons stops expressing the axonin-1 after crossing the Floor Plate (FP). But Fmn2 knockdown embryos showed

axonin-1 expression at the stage where the commissural neurons would have ideally crossed the FP.

So the main objective of the project was to characterize the role of Fmn2 in spinal cord development. The spinal cord showed Fmn2 enrichment between Stage HH19-22, the stage at which commissural neurons start crossing the midline. Due to these reasons we chose the commissural neuron to study the *in vivo* activity of Fmn2.

Commissural neurons are interneurons that connects the sensory neurons with the motor neurons. They are categorized into different groups based on their cell body position in the spinal cord and trajectory. We studies primarily dI1 commissural neurons in our experiments.

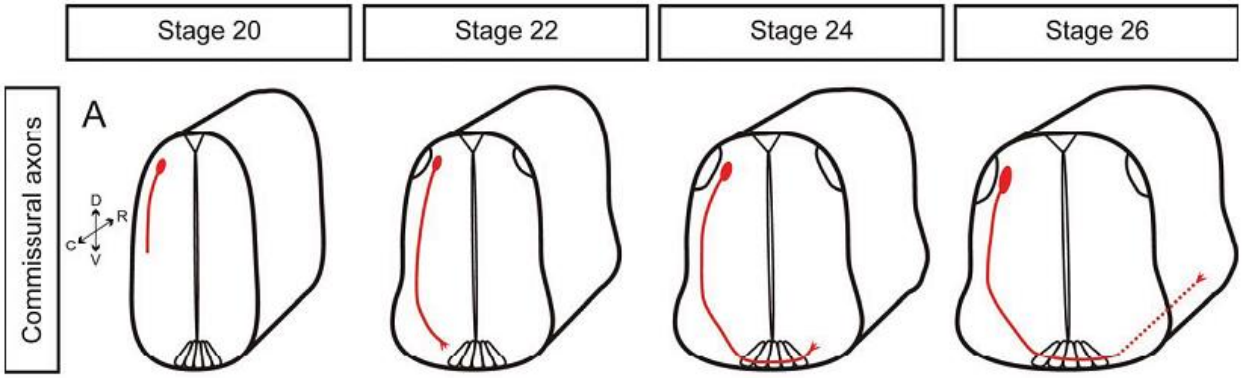

Fig 3. dI1 commissural neuron trajectory. dI1 commissural axons trajectory at different developmental stage of a chick embryo. Adapted from Neural Development (Joset et al., 2011)

The cellbodies of dI1 commissural neurons are located at the dorsal side near to the roof plate. In chick, by stage HH19 dI1 axons extends from their cell bodies and by stage HH24 axons cross the floor plate and start extending in the contra-lateral side after taking the characteristic sharp sigmoid turn (Joset et al., 2011)(Fig 3).

The dI1 trajectory is an outcome of several guidance cues (Kaprielian et al., 2000). The BMP released from the RP repels the dI1 axons from the dorsal side and it is then attracted towards the midline by Netrin and Shh released from FP. Cell adhesion

molecules like NrCAM guides the dI1 axons to cross the FP. While crossing the axons changes their expression pattern and become responsive to the repellent cues released by the FP such as Slits and Ephrins. Robo-Slit interaction prevents the post-crossing axons from re-entering the FP and repells the axons away from the midline. In the contralateral side the axons follow the Wnt gradient and moves longitudinally towards the rostral side.

4) Morpholinos and reporter plasmids

We used gFmn2_tb morpholino (MO) for knockdown the Fmn2 in the spinal cord. Morpholinos are synthetic oligonucleotides analogous to DNA and RNA (Eisen and Smith, 2008; Kos et al., 2003). In MOs the ribose ring is replaced by morpholine ring. They are generally a chain of 25 nucleotides which can undergo Watson-Crick base pairing. MOs are resistant to nucleases and are therefore remarkably stable. Since they do not carry a negatively charged backbone, they are less likely to interact non-specifically with other components of the cell and may be less toxic to the cell. These features makes them a suitable candidate for knock down studies. . Unlike DNA oligos they do not mediate RNAse H-dependent degradation of the mRNA. Rather they block the translation of the gene of interest by binding to the 5' end of the mRNA. Currently MOs that block the gene splicing is also available.

For identifying the Fmn2 knock down effect in the spinal cord we used reporter plasmids to label the axonal projections. In reporter plasmids the gene of interest will be attached to a promotor for expressing it in the cells or tissue. Specific promotors opens the opportunity to express the gene of interest only in a particular set of cells or tissues. Using an inducible promotor one can control the expression of the gene of interest for only a certain period of time.

In our experiments we used plasmids either with a generic promotor, CAG or a specific promotor Atoh1 or Math1. CAG is an actin promotor and it expresses the gene of interest in all cells, including neuronal and non-neuronal cells. Both Atoh1 and Math1 are dI1 commissural neuron specific markers (Reeber et al., 2008; Zisman et al., 2007).

The Math1 plasmid we used to label the dI1 axons work based on Cre-Lox system. Cre is a recombinase which cuts the DNA at the lox site. In dI1 neurons Cre removes the stop sequence and recombines the plasmid to express GFP.

The main objective of the project was to identify the role of Fmn2 in spinal neuronal circuit formation. We used the *in ovo* electroporation method to knock down Fmn2 using Morpholino and to label dI1 neurons using reporter plasmids such as CAG-GFP or Atoh1-mCherry. We saw midline crossing defects in Fmn2 depleted spinal cord and to study whether the defect is non-cell autonomous, morpholino resistant mFmn2 was expressed specifically in dI1 commisssural neurons, in the background of gFmn2_tb MO. Studies had reported that FH2 domain is sufficient for the activity of Formins. We cloned a truncated Formin, gFmn2_N with only the N-terminal region and electroporated into the spinal cord to study its effect in dI1 axonal projection.

Chapter 2

MATERIALS AND METHODS

1) *In ovo* electroporation

Fertilized chick eggs were incubated at 37^0C. Plasmid DNA or Morpholino was unilaterally electroporated into stage HH14/15 chick embryos at the thoracic level of the spinal cord (Hamburger and Hamilton, 1951). Fast-green or Phenol red was added enough to visualize the plasmid solution. Plasmid or MO injection was done using 1.5mm micro-capillary with pore size 50-100 µm. Pressure to the micro-capillary was given by micro-injector (time – 50 ms, pressure clear – 50 PSI, pressure injection – 10 PSI). Square-wave current (pulse number – 5, voltage - 21 V, pulse - 50 ms, pulse interval - 100 ms) was generated using a CUY21 SC (Nepagene) electroporator (electrode – CUY613p3, parallel holder – CUY580) (Krull, 2004). 0.5 ml of Dulbecco's Modified Eagle's Medium (DMEM) with PenStrep was added and kept in the incubator at 37^0C.

2) Open book preparation

Embryos were harvested at stage HH26 or HH28 and dissected according to the protocol (Avraham et al., 2010). The embryo was isolated from the egg and placed on a silicone rubber coated plate containing PBS. Head, tail and the visceral organs in the ventral side including the heart was removed from the embryo. Embryo was the stretched on his ventral side using pins to hold it and using a sharp needle longitudinal incision was made along the roof plate, from the rostral end to the caudal end of the spinal cord. Spinal cord was fixed by adding 500 µl of 4% formaldehyde into the lumen and keeping it for 15-30 minutes. Additional two longitudinal incisions were made at both sides of the spinal cord to detach the dorsal root ganglia away from the spinal cord. Detaching the floor plate from the tissue gave the intact spinal cord.The spinal cord between the limbs was again fixed in 4% formaldehyde for 15-30 minutes and mounted in PBS. The coverslips were sealed with silicone rubber gum.

3) Cryosectioning

Embryos were isolated from the egg at stage HH26 and removed the embryonic tissues to get the clean embryo. Embryos were fixed in 4% formaldehyde for 12 hrs. Fixed embryos were then consecutively treated with 10%, 20% and 30% sucrose for 12 hours and prepared cryomolds in OCT (optimum cutting temperature compound). Sectioning was done using cryotome (size - 15 µm, temperature - 17^0C). Sections were transferred to poly-L- lysine coated slides and mounted in glycerol.

4) Reporter plasmids and morpholinos

Plasmids or MO used for electroporation and their concentrations

a) CAG –GFP (from Addgene)
   Concentration used for electroporation - 500ng/µl.
   Contains the 1.7kb CAG promotor and GFP (green fluorescent protein)
b) Atoh1-Tau-mCherry (from Kaprielian's lab)
   Concentration used for electroporation - 1.5-2.5 µg/µl
   Contains the 1.4kb Atoh1enhancer, the β-globin basal promoter and Tau sequences fused to mCherry (Reeber et al., 2008).
c) Math1-Cre + CAG-lox-stop-lox-GFP (from Klar's lab)
   Concentration used for electroporation - 1.5-2.5 µg/µl
d) CAG-mFmn2_FL-GFP
   Concentration used for electroporation - 1.5 µg/µl
   Contains the 1.7kb CAG promotor and 4.7kb mFmn2 fused to GFP.
e) Atoh1-mFmn2_FL-GFP (generated in this study)
   Concentration used for electroporation - 2-2.5 µg/µl
   Contains the 1.4kb Atoh1enhancer, the β-globin basal promoter and 4.7kb mFmn2 fused to GFP
f) CAG-gFmn2_N1-GFP (generated in the lab by Abhishek)
   Concentration used for electroporation - 2-2.5 µg/µl
   Contains the 1.7kb CAG promotor and 1.56kb gFmn2_N.
g) Atoh1-gFmn2_N1-GFP (generated in this study)

Concentration used for electroporation - 2-2.5 µg/µl

Contains the 1.4kb Atoh1enhancer, the β-globin basal promoter and 1.56kb gFmn2_N.

h) CAG-gFmn2_N-GFP (generated in this study)

Contains the 1.7kb CAG promotor and 2.4kb gFmn2_N.

i) Control morpholino (from Genetools)

Concentration used for electroporation - 750 µM

Antisense sequence – 5' – CCTCTTACCTCAGTTACAATTTATA – 3'

Target – human beta-globin intron mutation that causes beta-thalassemia.

j) gFmn2_tb morpholino (from Genetools)

Concentration used for electroporation - 750 µM

Antisense sequence – 5' - TGCAATGCAGGCAATAAAAACCGTG - 3'

Target - 5' untranslated region of gFmn2 mRNA, 159-183.

For *in ovo* electroporation, the bacterias were incubated in 100ml nutrient broth for 16 hrs at 37^0C. Plasmids were isolated from the bacterial cultures using Qiagen Midi-Prep Kit. The isolated plasmids were dissolved in TE (Tris-EDTA, pH 8) buffer and concentrations were measured using Nanodrop machine.

5) Cloning of CAG-gFmn2_N-GFP

CAG-GFP plasmid was Sma1 digested overnight at 37^0C and treated with Calf Intestinal Alkaline Phosphatase (CIP) for 1 hr at 37^0C. The digested plasmid was run on a 0.8% agarose gel and the band for CAG-GFP (5.5 kb) was gel purified using Qiagen gel purification kit.

Total mRNA was isolated from a 5 day chick embryo using the standard protocol. Embryos were treated with trizol for the disruption of cell and cell components. Chloroform was added to separate nucleic acids from the homogenized mixture and they were recovered from the aqueous phase by precipitation with isopropyl alcohol. Precipitated nucleic acids were treated with DNase and sequential separation and precipitation was done to get the purified mRNA. cDNA library was generated using the reverse transcriptase MLV-RT with either of the primers (IDT):

a) Oligo dT

5’ – TTTTTTTTTTTTTTTTT – 3’

b) gFmn2_N (CAG) reverse

5’ – TGGTGGCGACCGGTGGATCCCCTACTGATTGGCTTGCATCCAGTG – 3’

PCR was used to amplify gFmn2_N from the cDNA library using the primers (IDT):

Forward – gFmn2_N (CAG) forward

5’- TCGACGGTACCGCGGGCCCCGCCACCATGGGGAATCAAGATGGGAAGCTA -3’

Reverse – gFmn2_N (CAG) reverse

The enzyme used for the PCR was AccuPrime Pfx (life technologies) and the reaction conditions were set based on the instructions given in the enzyme manual. PCR reaction mix was run on a 0.8% gel and gel purified the band for gFmn2_N (2.4kb) using Qiagen gel purification kit.

DH5α cells were transformed with the vector digest and the gFmn2_N PCR product using the standard protocol. For transformation, a cold shock (20min in ice) followed by a heat shock (10 min at room temperature and 1 hr at 37^0C) was given to the DH5α cells. The cells were plated on a Nutrient Agar plate containing the Ampicillin antibiotic and incubated at 37^0C for 16 hrs.

6) Cloning of Atoh1-mFmn2-GFP and Atoh1-gFmn2_N1-GFP

CAG-mFmn2-GFP or CAG-gFmn2_N-GFP was Sal1 digested overnight at 37^0C and treated with Calf Intestinal Alkaline Phosphatase (CIP) for 1 hr at 37^0C. The digested plasmids were run on a 0.8% agarose gel and the bands for mFmn2-GFP (8.6 kb) and gFmn2_N1 (6.1kb) were gel purified using Qiagen gel purification kit.

PCR was used to generate Atoh1 fragment with Sal1 sites, from Atoh1-mCherry, using the primers (Sigma):

Forward – Atoh1 (Sal1) forward

5’ - ACCTGGTCGACTCCAAGGTCCGGCAATGAAG – 3’

Reverse – Atoh1 (Sal1) reverse

5’ – GTACCGTCGACGCAGGCTAGAAGCAAATGTAAGC – 3’

The PCR product was PCR purified using Qiagen PCR purification kit and digested with Sal1, overnight at 37^0C. The digested Atoh1 was then PCR purified. The

digested vector and insert was ligated using Mighty Mix (Takara) 1:3 ratio (10 min at 25^0C). Standard protocols (as mentioned above) were then followed to transform DH5α cells with the ligated products. The cells were plated on a Nutrient Agar plate containing the Ampicillin antibiotic and incubated at 37^0C for 16 hrs.

Screening of Atoh1-gFmn2-GFP using PCR:

Forward primer – 5'- GGCAGAGTTTACAGAAGCC – 3'

Reverse primer – 5' – GTTTTGATGTAACAAGGATTAATTAGATAGGGCTTAAAGC - 3'

7) Imaging

Plasmid expression in the embryo was captured using an epi fluorescence stereo microscope. Cryosection images were captured on Zeiss Apotome at 10x magnification using GFP filter.Confocal images of spinal open-book were acquired on LSM780 (Zeiss) at 20X magnification using mCherry and EGFP filters. Confocal imaging was done by 3 X 3 tiling and Z-stack with a distance of 5 µm. Parameters that had kept constant while imaging, pixel – 1024 x 1024, 12 bit, scan speed – 6 and frame average – 2. Images were analyzed using ImgeJ software.

8) Quantification

a) Pre and Post crossing intensity

An area of 200 µm X 100 µm was used to calculate the raw intensity of an image in a z-stack. The total intensity was then calculated by adding the area intensity in each image of a z-stacks having the post-crossing or pre-crossing axons. For pre crossing and post crossing axons the area was chosen at a distance of 100 µm and 50 µm respectively from the FP (Fig 7.C)

b) Pre and Post crossing axonal tract number.

Axonal tracts were counted for a distance of 100 µm in the maximum intensity projection of the z-stack image. For pre crossing and post crossing axons, the length was chosen at a distance of 100 µm and 150 µm from the FP respectively (Fig 7.F).

The quantified data was plotted and analyzed using GraphPad Prism software. Unpaired T-test, two tailed - was used for the statistical analysis of the data.

Chapter 3

RESULTS

1) *In ovo* electroporation can label populations of dI1 commissural neurons:

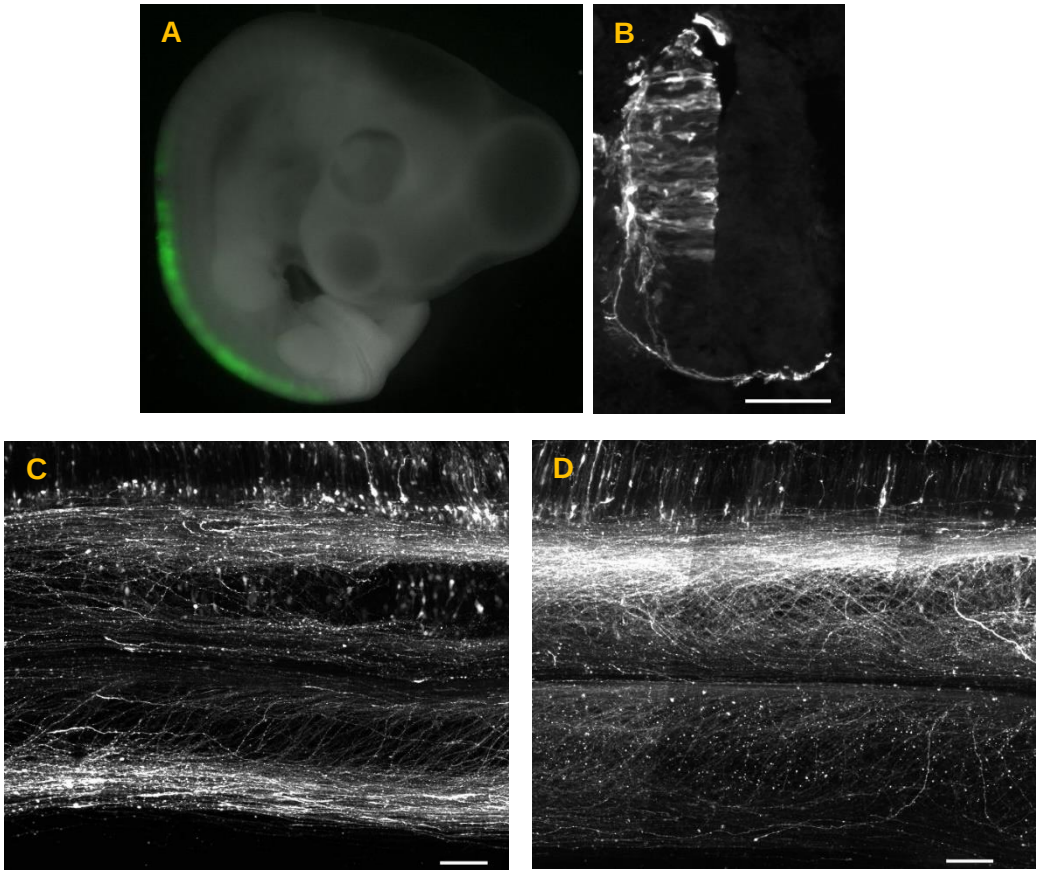

Fig 4. Reporter plasmids label the dI1 axonal projection. A) Chick embryo electroporated with Math1- Cre + CAG-lox-stop-lox-GFP, (Stage HH26). B) Cryosection of spinal cord expressing Math1-Cre + CAG-lox-stop-lox in the dI1commissural neurons (Stage HH26). Open-book of spinal cord expressing C) Math1- Cre + CAG-lox-stop-lox-GFP and D) Atoh1-mCherry in the dI1commissural neurons (Stage HH28). Scale bar-100µm

In ovo electroporation was used to label the dI1 commissural neurons. In control experiments to establish the procedure, HH stage 14/15 chicken embryos were unilaterally electroporated with CAG-GFP. CAG is a generic promotor and the plasmid expresses in both neuronal and non-neuronal cells. Embryos showed GFP expression in the spinal cord after 48-53 hrs of incubation (Fig 4.A).

Same procedures were followed to label the dI1 commissural neurons using two sets of plasmid, i) Atoh1-mCherry and ii) Math1-Cre + CAG-lox-stop-lox-GFP. Cryosection and open-book images of spinal cord electroporated with either of the plasmids showed the trajectory of dI1 commissural neurons (Fig 4.B, C, D). In the ipsilateral side, the dI1 axons extended from the dorsal cell bodies to the midline and crossed the FP. The post-crossing axons in the contralateral side took the characteristic sharp sigmoid turn to extend longitudinally towards the rostral side.

2) Fmn2 knockdown cause midline crossing defects in dI1 commissural neurons

The standardized electroporation and open-book procedures were followed for studying the Fmn2 activity in axonal projection. Fmn2 was knocked down in the spinal cord by electroporating gFmn2_tb MO, which binds to the 5' UTR of gFmn2 mRNA and thereby blocks the translation. Experiments to check the knock down efficiency has shown that gFmn2_tb MO decreases the Fmn2 levels in the spinal cord (Sahasrabudhe, 2015).

The spinal neurons electroporated with CAG-GFP and gFmn2_tb MO showed a trajectory similar to the control MO treated neurons (Fig 5.A, B). Since CAG is a strong, generic promoter which expresses in all cell types (neuronal and non-neuronal), it lacks the resolution to identify whether some specific class of neurons are affected by the depletion of Fmn2.

Studies in our lab has shown Fmn2 enrichment in the chick spinal cord during HH19-22. This is the stage where commissural neurons start crossing the FP. So we chose dI1 commissural neurons to study the Fmn2 activity in axonal motility and spinal cords were electroporated with Atoh1-mCherry and morpholinos.

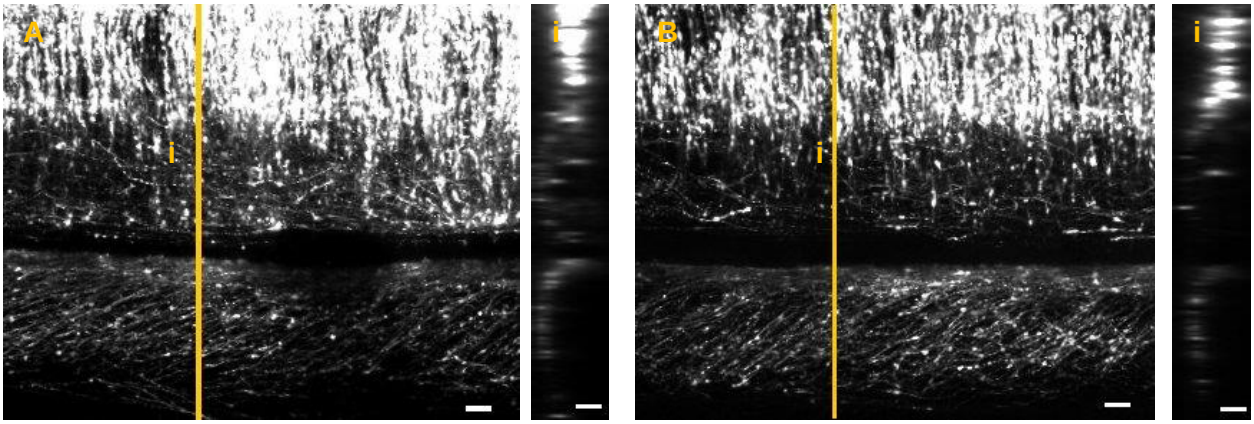

Fig 5.Spinal cord electroporated with CAG-GFP and morpholinos. CAG-GFP expression in spinal co-electroporated with A) Control MO (n=6), B) gFmn2_tb MO (n=5). Both control MOand gFmn2_tb MO treated spinals showed similar phenotype. i) Spinal in yz plane at the line I marked in A and B. (Stage HH26). Scale bar-50µm

Fmn2 knock down caused extensive midline crossing defects in the dI1 neurons compared to wild type (Fig 6.B, C and D). The knockdown phenotypes were categorized into 'non-crossing (nc)' and 'defective crossing (dc)'. In non-crossing phenotype, axons crossed the FP but failed to extend further (Fig 6.C). In defective crossing, axons that moved longitudinally failed to take the characteristic sharp sigmoid turn and remained closer to the floor plate (Fig 6.D). In both the knock down phenotypes, a small number of post-crossing axons moved straight without taking any turn (Fig 6.C, D). Only 15 percentage of gFmn2_tb MO treated spinal cord showed the wild type phenotype (Fig 6.B). Whereas 65 percent of the control_MO treated embryos showed the wild type phenotype (Fig 6.A, B).

To make sure that the knockdown phenotypes were not due to stage defect, morphology of the embryos were used as a criteria for identifying the stage. After 4.5 -5 days of incubation at 37^0C, embryos were analyzed for the morphology. At stage HH26 embryos have pigmented eyes and the limbs are of equal length and width. The contour of digital plate is rounded with first three toes distinct. Both the control MO and gFmn2_tb MO treated embryos had the same characteristic morphology of stage HH26.

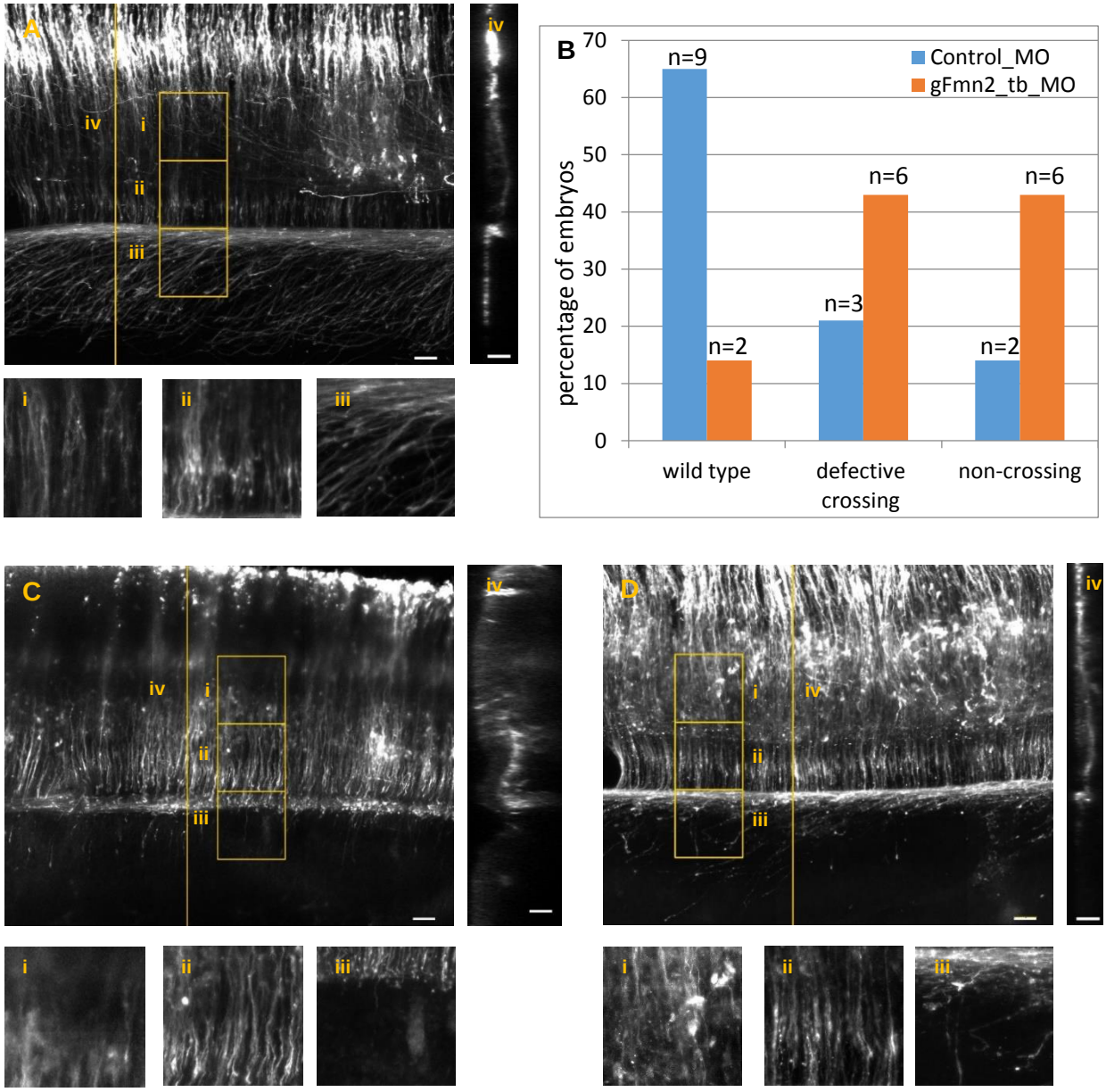

Fig 6. Fmn2 knockdown cause midline crossing defect in dI1 neurons. Atoh1-mCherry expression in spinal co-electroporated with A) Control MO, C and D) gFmn2_tb MO. A) Wild type phenotype where the post-crossing axons take the characteristic sharp sigmoid turn B) percentage of embryos showing the phenotypes after control_MO and gFmn2_tb MO treatment C) 'non-crossing' knockdown phenotype D) 'defective crossing (dc)' knockdown phenotype. DI1 axonal trajectory in the i) ipsilateral side ii) midline and iii) contralateral side iv) spinal in yz plane at the line iv marked in A, C and D . (Stage HH26) Scale bar-50µm

Use of these criteria allowed to compare spinal cords from development stage-matched embryos.

For quantifying the phenotypes mCherry intensity was considered as an indicator for the number of axons. The contralateral to ipsilateral intensity ratio was calculated to get an estimate of percentage of axons projecting in the contra-lateral side (Fig 7.A, B). Taking the ratio will eliminate problems due to differences in transfection efficiency between the spinal cords. The ratios were calculated after background subtraction. For the checking the accuracy of intensity based quantification only the spinal cord showing wild tpe phenotype has been considered in controls and non-crossing phenotype in Fmn2 knockdown. Fmn2 knock down spinals did not show a significant decrease in the ratio (Fig 7.C). In controls the ratio was 0.77 and in gFmn2_tb MO treated spinals the ratio was 0.15.

The quantification based on signal intensity was relatively coarse grained and also subject to errors introduced by variations in the background signal. Uniform background subtraction, as employed above, is expected to be inadequate to address the variation in the signal intensity. The occasional presence of saturated regions in the image may have distorted the ratio. These could be the reason for getting a non-zero ratio in the non-crossing phenotype.

To circumvent this confound, the axonal tracts entering the FP and the tracts extending into the contralateral side were directly counted (Fig 7.D, E). The contralateral to ipsilateral ratio was calculated to estimate the percentage of axons that succeed in crossing the floor plate and extending into the contralateral side. For this quantification, both wild type and defective phenotype were included in control MO treated spinal cords and gFmn2_tb treated spinal cords. Fmn2 knock down spinal cord showed a significant decrease in the crossing ratio ($p=0.0166$) (Fig 7.F). In Fmn2 knock down spinal cords the crossing ratio was 0.18, whereas in controls the ratio was 0.44. Quantification based on the axonal tract eliminated the problems like variation in transformation efficiency between embryos and cell death caused by Fmn2 knock down.

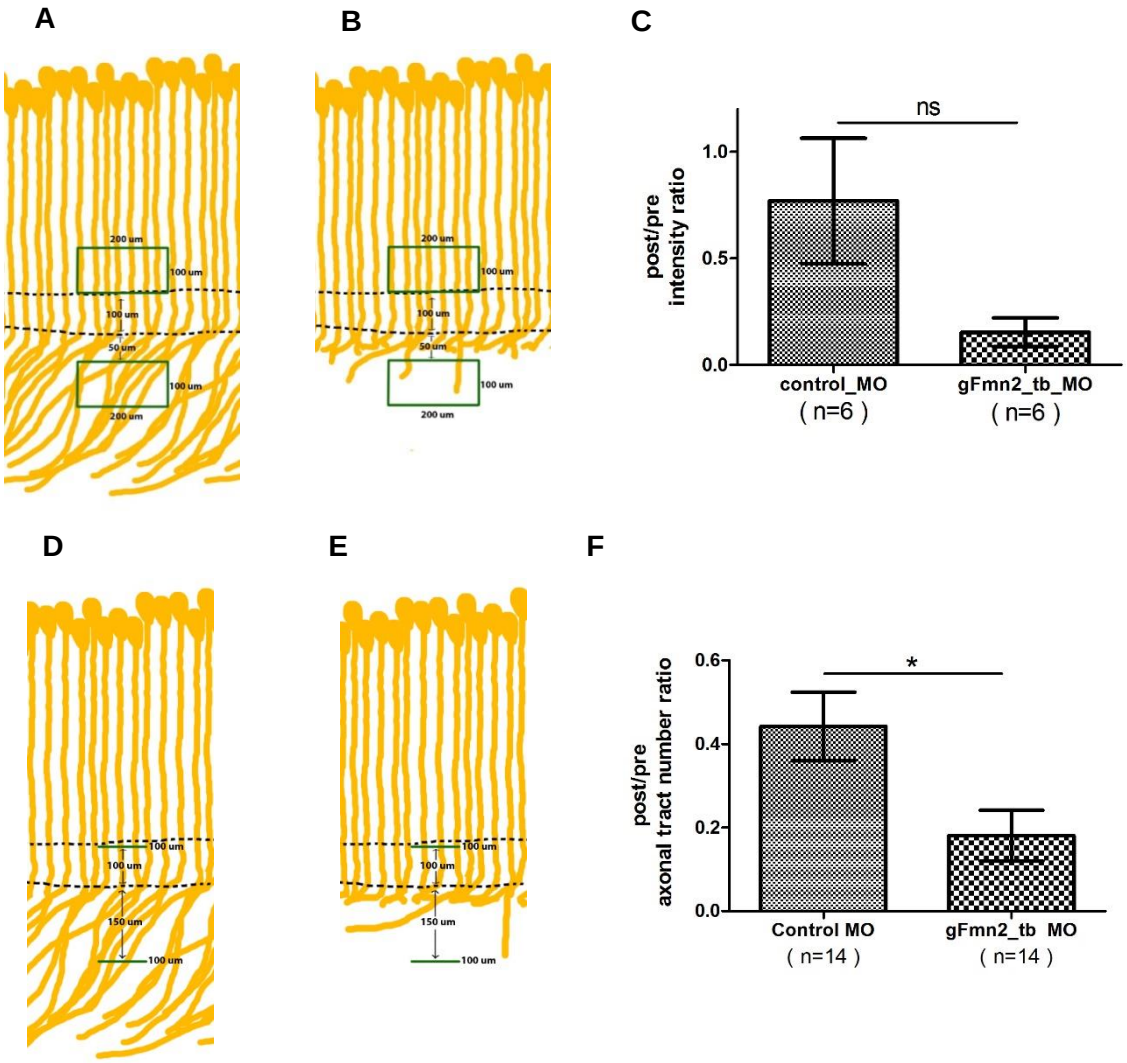

Fig 7. Quantification of the morpholino treated spinal cords. Schematic of measuring the mCherry intensity in A) Control MO and B) gFmn2_tb MO treated spinals (green box). C) The ratio of fluorescence intensity in post- and pre -crossing axons, in the control and gFmn2_tb MO treated spinals (p=0.0686) (unpaired t-test, two tailed). Schematic of counting the number of axonal tracts in D) Control MO and E) gFmn2_tb MO treated spinals (green line). F) The ratio of the number of post- and pre -crossing axonal tracts, in the control and gFmn2_tb MO treated spinals (* p=0.0166 unpaired t-test, two tailed; error bar- standard error in mean)

Embryos were also co-electroporated with gFmn2_tb MO and Math1-Cre + CAG-lox-stop-lox-GFP. Math1 positive dI1 commissural neurons showed a similar defective crossing phenotype in Fmn2 depleted spinal cords (Fig 8). Axons that crossed the floor plate failed to take the characteristic sharp sigmoid turn and remained close to the midline.

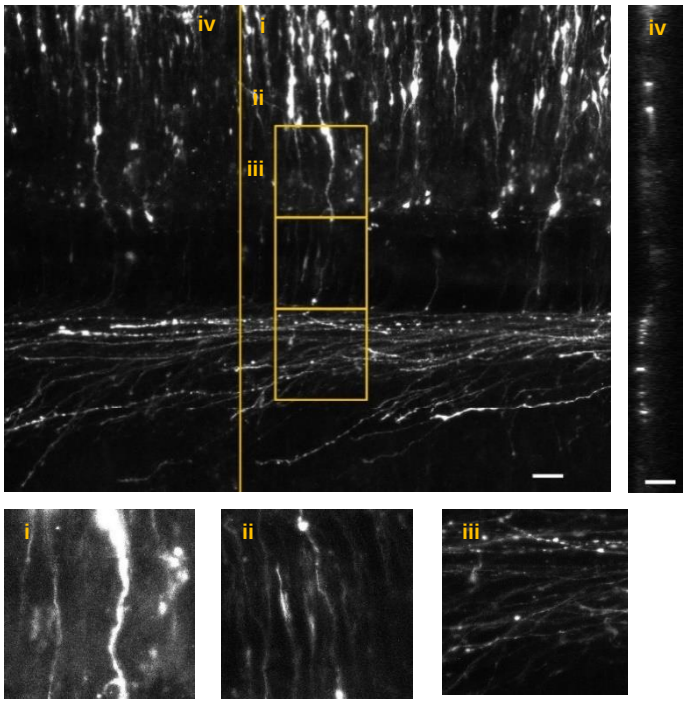

Fig 8. Fmn2 knockdown cause defective crossing in Math1 positive dI1 neurons. Math1-Cre + CAG-lox-stop-lox-GFP expression in spinal co-electroporated with gFmn2_tb MO. Math1 positive dI1 neurons showed defective crossing. Dl1 axonal trajectory in the i) ipsilateral side ii) midline and iii) contralateral side iv) spinal in yz plane at the line marked iv. (Stage HH26). Scale bar-50µm

3) Fmn2 activity is required in the dI1 commissurals for floor plate crossing

Electroporation of gFmn2_MO introduces the reagent in all neuronal and non-neuronal cell populations in the developing spinal cord where it blocks Fmn2 translation.

Thus the midline crossing defects in the Fmn2 knockdown neurons could be due to the requirement of FMn2 activity in non-neuronal and/or non dI1 cells.

To test whether Fmn2 activity is required non-cell-autonomously in the dI1 commissural neurons, a rescue strategy was developed. It involves the overexpression of morpholino resistant mFmn2, specifically in the dI1 neurons, in the background of electroporated gFmn2_tb MO. Since the gFmn2_tb is sequence specific it would not bind to the mFmn2 mRNA. Thus mFmn2 will be MO resistant and can polymerize the actin filaments even in the presence of gFmn2_tb MO. Both mFmn2 and gFmn2 have the evolutionarily conserved FH1 and FH2 domains. The function of Fmn2, promoting actin nucleation and polymerization in the cells, is conserved in mouse and chick. Hence, in the gFmn2_tb MO treated spinal cord the mFmn2 can substitute the function of gFmn2.

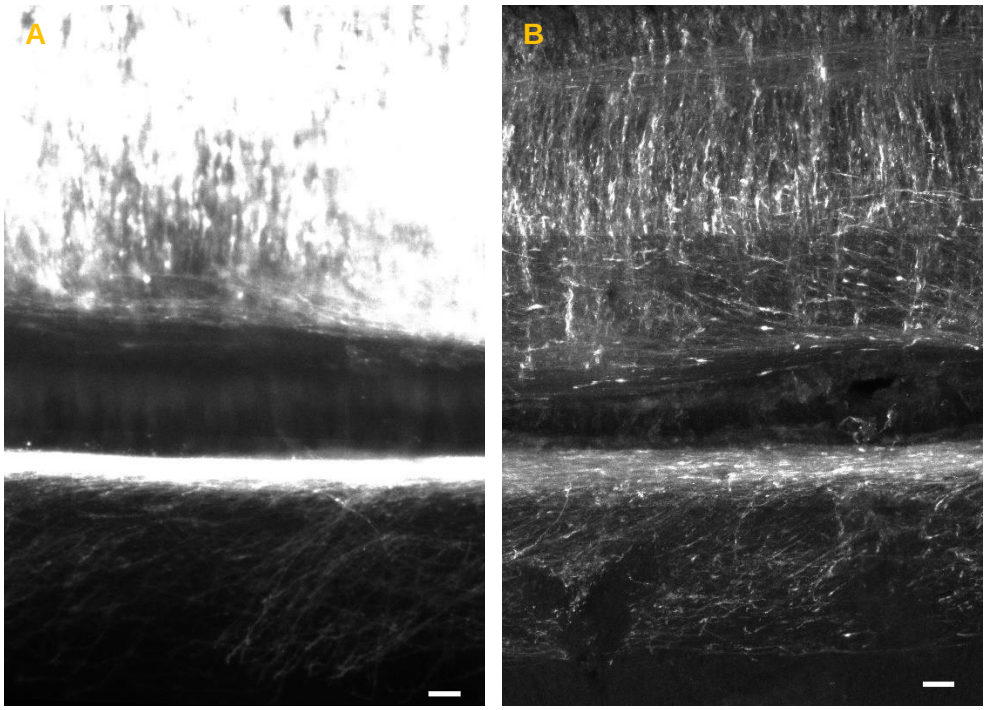

Fig 9. Expression of CAG-mFmn2-GFP. Spinal cord expressing A) CAG-GFP, B) CAG-mFmn2-GFP. (Stage HH26) Scale bar-50µm

.

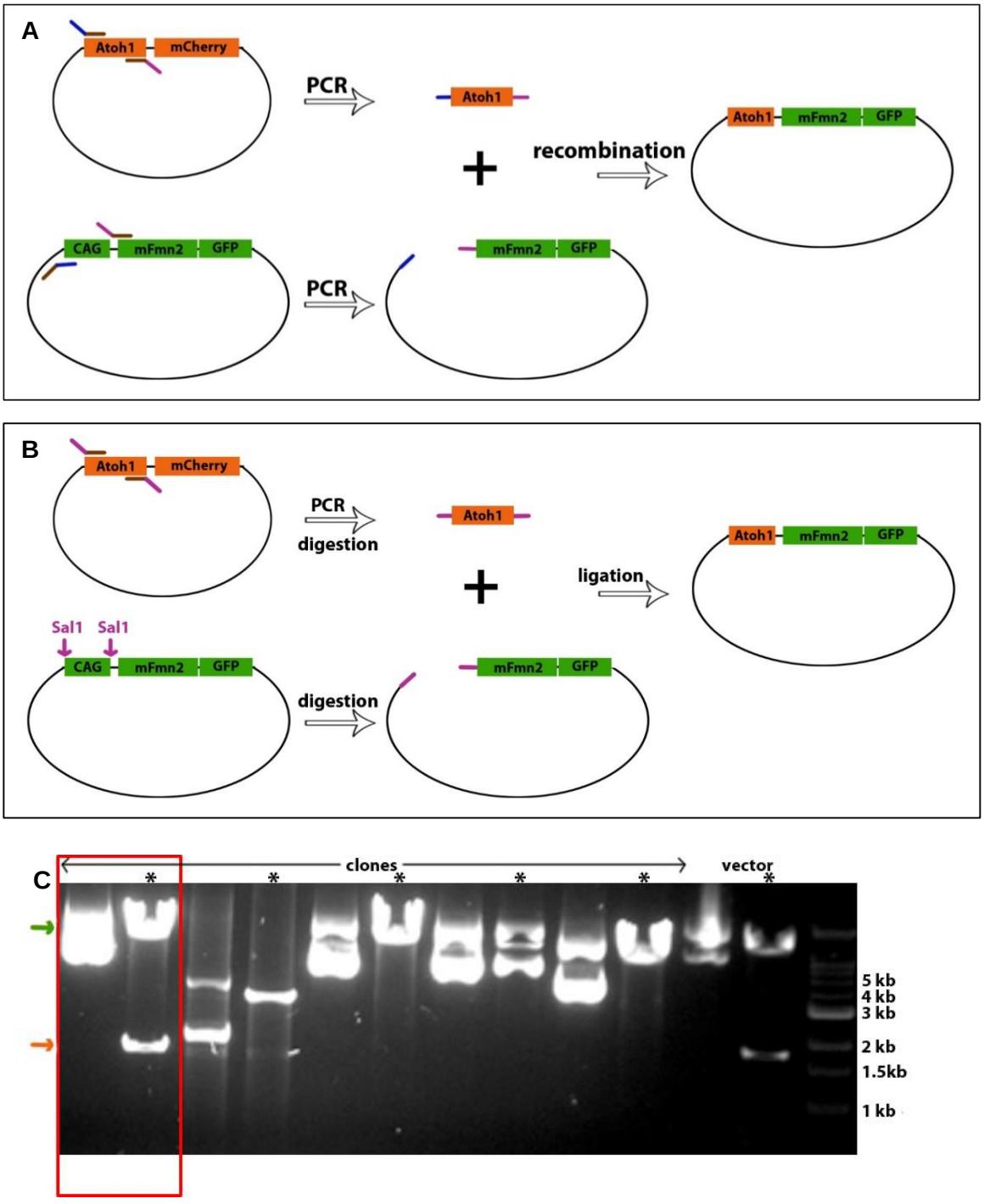

Fig 10. Cloning of Atoh1-mFmn2-GFP. Schematic of Atoh1-mFmn2-GFP cloning using A) Homologous recombination, B) digestion and ligation. C) Sal1 digestion of the Atoh1-mFmn2-GFP clone (red box). (* digestion products, left to the * - undigested plasmid). Vector backbone ~ 9kb (green arrow), atoh1 ~ 1.5kb (red arrow)

To show that the knockdown phenotype is intrinsic to dI1 commissural neurons, mFmn2 was cloned under the control of the Atoh1 enhancer. Since the plasmid is driven by Atoh1, mFmn2 will be expressed only in the dl1 commissural neurons. Several strategies were tried to get the clone.

In one strategy homologous recombination was used to replace the CAG in the plasmid with Atoh1 (Fig 10.A). PCR was used to generate Atoh1 fragment from Atoh1-mCherry and linearized vector (excluding CAG) from CAG-mFmn2-GFP. Competent cells were transformed with, Atoh1 fragment having vector overlapping region and the vector having Atoh1 overlapping region. Screening didn't show up any positive clone. Since the vector size was 8.5kb, it is possible that the PCRs failed to amplify the fragment.

In another set of experiments, PCR was used to amplify the Atoh1 fragment flanked with primer introduced Sal1 sites from Atoh1-mcherry (Fig 10.B). Concurrently, CAG-mFmn2-GFP was digested with Sal1 to get the linearized vector excluding CAG. The digested PCR product and the vector was ligated and transformed. Colony screening using Sal1 digestion identified a positive clone (Fig 10.C). Sequencing results also conformed the clone to be Atoh1-mFmn2-GFP.

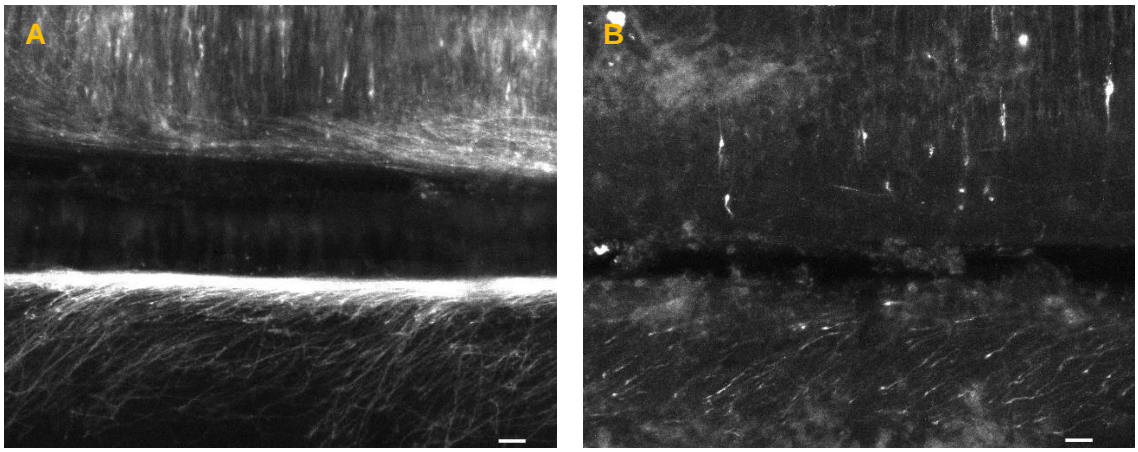

Fig 11. Expression of Atoh1-mFmn2-GFP. Spinal cord expressing A) Atoh1-mCherry, B) Atoh1-mFmn2-GFP. (Stage HH26) Scale bar-50µm

Spinal cords electroporated with Atoh1-mFmn2-GFP showed expression in the dI1 commissural neurons. The neurons displayed wild type phenotype, were the axons crossed the floor plate and extended longitudinally in the contralateral side by taking a sharp sigmoid turn (Fig 11.A, B). Thus overexpression of mFmn2 did not interfere with the endogenous gFmn2 activity to affect axonal trajectories.

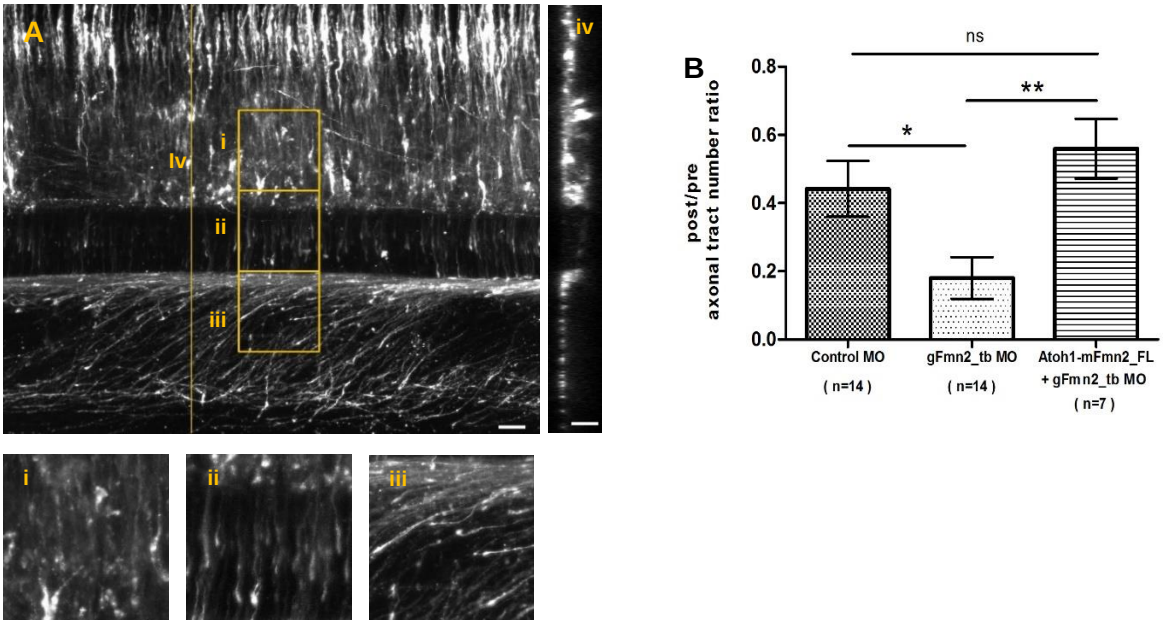

Fig 12. mFmn2 rescue the gFmn2 depleted dI1 axons from midline crossing defects. A) Atoh1-mCherry expression in spinal co-electroporated with gFmn2_tb MO and Atoh1-mFmn2-GFP. B) Post-crossing to pre-crossing axonal tract ratio in the MO treated spinals and mFmn2 rescue.DI1 commissural trajectory in the i) ipsilateral side ii) midline and iii) contralateral side iv) spinal in yz plane. (Stage HH26). Scale bar-50µm. (* p=0.0166, ** p=0020 unpaired t-test, two tailed; error bar- standard error in mean).

Atoh1-mFmn2-GFP was co-electroporated along with the morpholinos and Atoh1-mCherry in the spinals. Neurons co-electroporated with gFmn2_tb MO, Atoh1-mCherry and Atoh1-mFmn2-GFP showed post-crossing trajectories similar to control_MO treated neurons (Fig 12.A). The post-crossing to pre-crossing axonal tract ratio was also not significantly different from the control_MO treated spinals (Fig 12.

B).Whereas the ratio was significantly different from the spinals treated only with the gFmn2_MO (p=0020). So the overexpression of mFmn2 rescue the midline crossing defects of these neurons induced by morpholino mediated gFmn2 knock down. This suggests that the midline crossing defects of dI1 commissural neurons upon Fmn2 depletion was largely due to cell intrinsic activity of Fmn2 in these cells. This data also underscores the evolutional conserved nature of Fmn2 function in these neurons as the mouse ortholog is able to rescue axon guidance of dI1 commissural neurons in the chick spinal cord.

4) Overexpression of gFmn2 N-terminus fragment (gFmn2_N1) cause midline crossing defect in dI1 comissural neurons

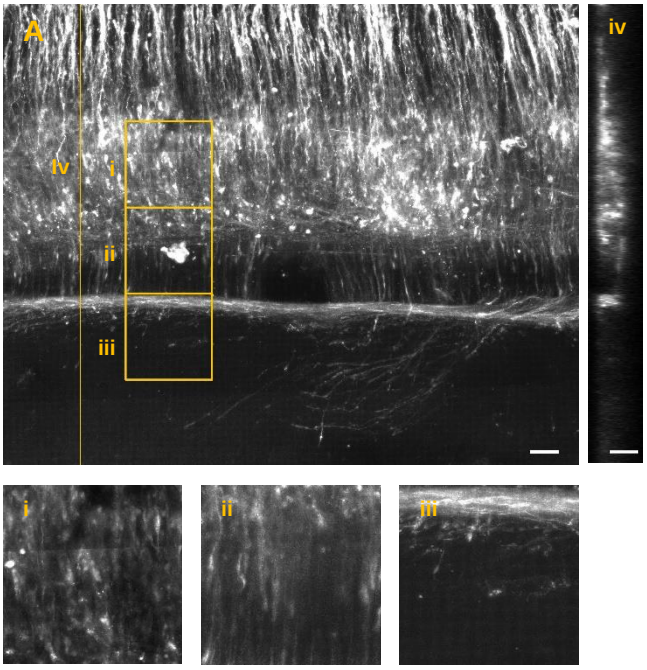

Fig 13. CAG-gFmn2_N1 cause midline crossing defect in dI1 axons A) Atoh1-mCherry expression in spinal co-electroporated with CAG-gFmn2_N1-GFP. B) Post-crossing to pre-crossing axonal tract ratio. Dl1 commissural trajectory in the i) ipsilateral side ii) midline and iii) contralateral side iv) spinal in yz plane. (Stage HH26) Scale bar-50µm

FH1 and FH2 domains at the C terminus of the formins, including Fmn2, are the profilin and actin interacting domains respectively (Fig 2). These domains play a crucial role in actin nucleation and polymerization by formins. So formin with only the N-terminus (gFmn2_N) will be non-functional. Since formins function as homo-dimers, overexpression of gFmn2_N may act as a dominant negative by dimerizing with endogenous gFmn2. A dimer of gFmn2_N and endogenous gFmn2 could potentially be non-functional as it results in an incomplete FH2 ring.

For cloning the gFmn2_N, total mRNA was isolated from a 5 day chick embryo. mRNAs were reverse transcribed with poly dT oligo to generate a cDNA library. PCR with specific primers was used to produce the two fragments of N and it was then joined using PCR. Competent cells were transformed with the PCR fragment and the linearized vector to get the CAG-gFmn2_N-GFP clone. (Cloning was done by Abhishek). Sequencing of gFmn2_N showed a 167 nucleotide deletion at 1562 and 88 nucleotide insertion at 1772. A stop codon was formed due to the deletion resulting in the translation of only the initial 530 amino acids and not translating the C-terminus GFP. This truncated form of gFmn2_N is indicated as gFmn2_N1 in the following sections.

Spinal cords co-electroporated with CAG-gFmn2_N1-GFP and Atoh1-mCherry showed defects in midline crossing (Fig 13. A). Similar to knock down phenotypes, some post crossing axons failed to extend. Post-crossing axons that extended longitudinally did not take the characteristic sharp sigmoid turn and remained closer to the midline. A few of the axons moved straight in the contralateral side.

To test if the dominant negative like phenotype is a non-cell-autonomous effect of expression in dI1 commissural neurons, Atoh1-gFmn2_N1-GFP was generated using a cloning strategy similar to Atoh1-mFmn2-GFP (Fig 10.B). Atoh1 with Sal1 overhangs were generated by PCR from Atoh1-mCherry, and CAG-gFmn2_N1-GFP was digested with Sal1 to obtain a linearized vector excluding the CAG. The two fragments were ligated and transformed to get colonies. Colony screening using Sal1 digestion and PCRs showed a positive clone (Fig 14 A, B). Sequencing results also confirmed the clone to be Atoh1-gFmn2_N1-GFP.

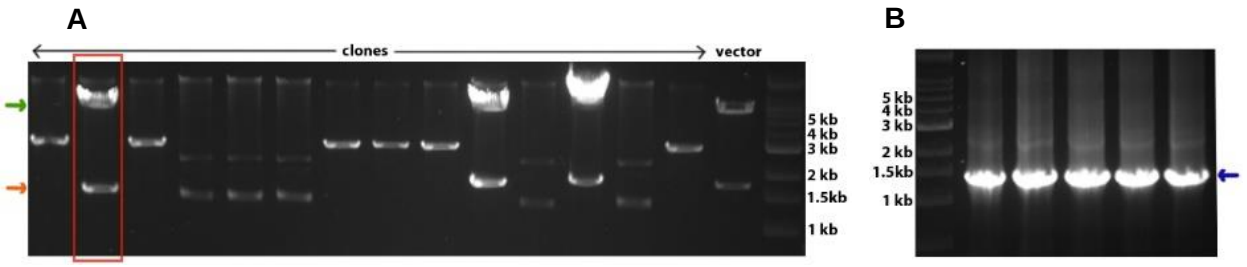

Fig.14 cloning of Atoh1-gFmn2_N1-GFP. A) Sal1 digestion of the Atoh1-gFmn2_N1-GFP clone (red box). Vector backbone ~ 9kb (green arrow), atoh1 ~ 1.5kb (red arrow) B) Gradient PCR of Atoh1-gFmn2_N1-GFP for gFmn2_N1 using Atoh1 forward and gFmn2_N1 reverse. gFmn2_N1 ~ 1.5kb (blue arrow)

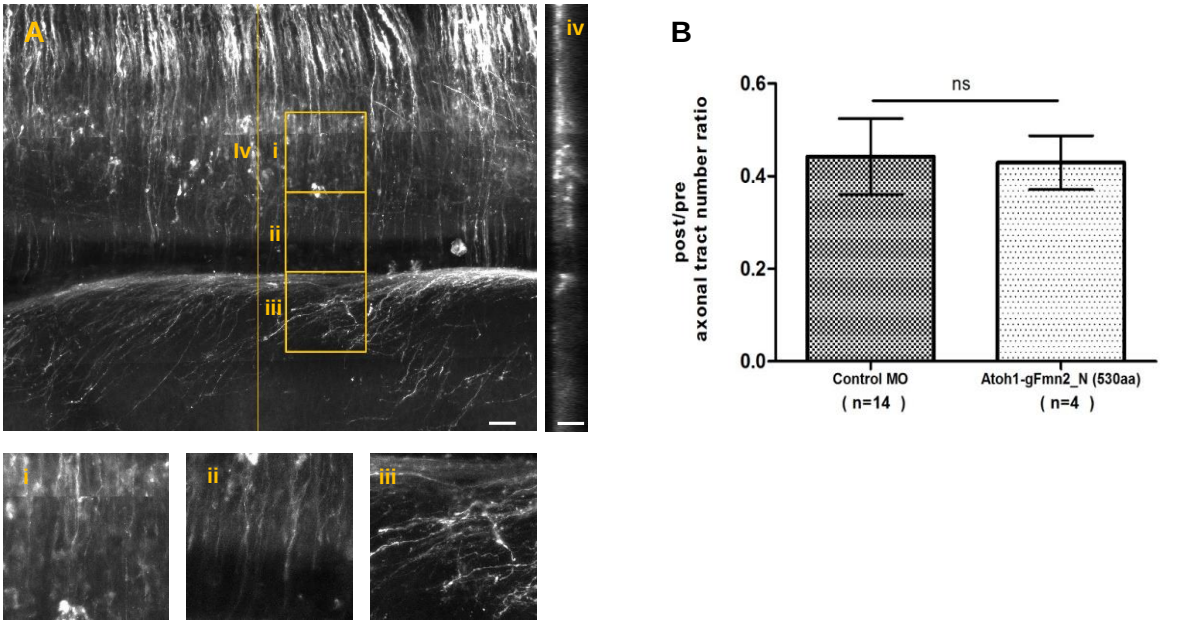

Fig 15. Atoh1-gFmn2_N1 cause midline crossing defect in dI1 axons. A) Atoh1-mCherry expression in spinal co-electroporated with Atoh1-gFmn2_N1-GFP. B) Post-crossing to pre-crossing axonal tract ratio. Dl1 commissural trajectory in the i) ipsilateral side ii) midline and iii) contralateral side iv) spinal in yz plane. (Stage HH 26) Scale bar-50µm

The spinal cords co-electroporated with Atoh1-gFmn2_N1-GFP and Atoh1-mCherry showed some defects in the post-crossing axons (Fig15 A). But the ratio of post-crossing to pre-crossing axonal tracts didn't show a significant difference as compared to the wild type (Fig15 B). Thus, even though there is defect in the trajectories, the percentage of axons crossing and extending in the contra-lateral side doesn't change much.

To overcome the problem due to deletion and insertion, cloning of the intact gFmn2_N was re-initiated. Total mRNA was isolated from a 5day old chick embryo and used to make the cDNA library. PCR with specific primers was then used to amplify the gFmn2_N as a single fragment from the cDNA pool. The primers used for the PCR had vector overlapping regions. CAG-GFP was digested with Sma1 to get a linearized vector. *E.coli* was transformed with the vector and the insert to get the clones. Sequencing identified 3 positive colonies for the CAG-gFmn2_N-GFP. These clones will be used to get the Atoh1 driving gFmn2_N and will be expressed in the spinal cord to study the gFmn2_N effect in dI1 axonal projection.

5) Cloning of gFmn2_C and gFmn2_FL

Formins such as mDia have DAD domain at the N-terminus, which regulates its activity. Studies also suggest that truncated formins with only the C-terminus can act as a constitutively active formin. Presence of a regulatory domain is not identified in Fmn2. Based on homology gFmn2_ C (including FH1 and FH2 domains and excluding the N-terminus) could be consecutively active. For cloning gFmn2_C cDNA library was prepared similar to gFmn2_N. PCR using specific primers were used to amplify the gFmn2_C from the cDNA pool. The primers had Age1 restriction site. The PCR product and CAG-GFP were digested using Age1. The digested vector and insert was ligated and transformed to get colonies. Colony screening by Age1 digestion showed the right size bands in one clone. But the sequencing identified that the clone was not gFmn2_C, rather it was some unknown noncoding sequence.

Since the gFmn2_C region has a lot of GC rich region the primer slippage might have occurred during the PCR. This could be the reason for getting multiple bands in the PCR and finally the wrong clone. To increase the specificity, forward primer with 40 nucleotides was used to amplify the gFmn2_C from the cDNA library. CAG-GFP was digested with Sma1 and Age1 to get a linearized vector with a blunt end and a sticky end. PCR product was digested with Age1. The vector and insert were ligated and transformed to get the colonies. Screening of the colonies is in progress.

Chapter 4

DISCUSSION

1) *In ovo* electroporation using the dI1 specific reporter plasmids labels the axonal trajectory reproducibly

Chick embryos has served as a model system for developmental studies due to its easy access for surgical manipulations and a wealth of information on chicken embryogenesis. Introduction of *in ovo* electroporation has made the chick embryos an ideal system to study neuronal development (Muramatsu et al., 1997). *In ovo* electroporation can be successfully used for gain-of function and loss-of function studies (Krull, 2004). Protein knock-down experiments using morpholinos and RNAi can be done efficaciously by this method (Reeber et al., 2008; Kos et al., 2003; Nakamura et al., 2004).

The chick embryo is also well suited for investigation into the development of neuronal circuits, especially when combined with tracing specific axonal tracts. Injecting lipophilic dyes like DiI into the neurons stains the membrane and labels the trajectory of the axonal tracts. Since the method relies on manual injection, it doesn't ensure that the same subset of neurons were marked reproducibly. This can be overcome by genetically marking the neuronal cell types using reporter plasmids. *In ovo* electroporation serves as an efficient method to deliver the reporter plasmids into the spinal neurons. Electroporating the embryos with a generic marker, CAG-GFP labelled the neuronal and non-neuronal cell populations in the spinal cord. To specifically label the dI1commissural neurons we used either Atoh1-mCherry or Math1-Cre+CAG-lox-stop-lox-GFP. Both the plasmids marked dI1 cellbodies at the dorsal side and the pre and post crossing axons. Similar to the dI1 trajectories published in the papers, we saw the axons extending from the dorsal cell bodies to the midline in the ipsi-lateral side and

post-crossing axons taking the characteristic sharp sigmoid turn and extending longitudinally in the contralateral side.

2) Fmn2 knock down cause defective midline crossing in dI1 commissural neurons

Electroporation of the spinal cords with gFmn2_tb MO and CAG-GFP showed a phenotype similar to the control MO treated spinal cord. Since CAG is a strong, generic promoter which expresses in all cell types (neuronal and non-neuronal), it lacks the resolution to identify whether some specific class of neurons are affected by the depletion of Fmn2.

The qRT PCR data from the lab shows an increase in the level of actin nucleators, including Spire2 and Fmn2, during stage HH19-22.This is the stage were the commissural neurons cross the midline and start extending in the contralateral side. Embryos electroporated with gFmn2_tb MO had extensive defects in midline crossing. 43 percent of the embryos showed non crossing phenotype, were the axons cross the midline but fail to extend further. Another 43 percent showed a defective crossing, were the axons that moved longitudinally failed to take the characteristic sharp sigmoid turn and remained closer to the floor plate. The degree of knockdown by gFmn2_tb MO was checked by western blot analysis and it confirms that the Fmn2 protein levels were reduced in gFmn2_tb MO electroporated spinal cords (Sahasrabudhe, 2015).

To make sure that the knockdown phenotypes were not due to stage defect, morphology of the embryos were used as a criteria for identifying the stage. This allowed us to compare spinal cords from developmental stage-matched embryos.

Both the quantification based on the axonal tract numbers and mCherry intensity shows a significant difference between the control and the gFmn2_tb MO treated spinal cords. The quantification based on signal intensity was relatively coarse grained and also subject to errors introduced by variations in the background signal. Uniform background subtraction was inadequate to address the variation in the signal intensity and the occasional presence of saturated regions in the image distorted the ratio. These

could be the reason for getting a non-zero ratio in the non-crossing phenotype. Due to these reasons signal intensity based quantification was not continued further.

In Fmn2 knock down spinal cords the ratio of the number of post- and pre - crossing axonal tracts was 0.18. Among the axons that entered the floor plate, only 18 percentage of them succeeds in extending in the contra lateral side. In controls the ratio was 0.44, which means a 250 percent increase in post-crossing axons as compared to Fmn2 knockdown embryo. Quantification based on the axonal tract eliminated the problems like variation in transformation efficiency between embryos and cell death caused by Fmn2 knock down.

3) Fmn2 activity is required in the dI1 commissurals for floor plate crossing

Electroporation introduces the gFmn2_tb MO in all neuronal and non-neuronal cell populations in the developing spinal cord where it blocks Fmn2 translation. Thus the knockdown phenotypes could be due to the requirement of Fmn2 activity in non-neuronal and/or non dI1 cells. In the presence of atoh1 driven mFmn2, the gFmn2_tb MO treated dI1 axons crossed the midline and extended in the contralateral side (Fig 12). This suggests that the midline crossing defects seen in the Fmn2 knockdown neurons were due to the loss of Fmn2 activity in the dI1 neurons. The ratio of the number of post- and pre-crossing axonal tracts (0.56) was not significantly different from the control MO treated embryos but showed a significant difference between the gFmn2_tb MO treated embryos (p=0020).

Both mFmn2 and gFmn2 have evolutionarily conserved FH1 and FH2 domains, which are essential for formin mediated actin nucleation and polymerization (Leader and Leder, 2000). dI1 neurons expressing the mFmn2 showed trajectories similar to the control (Fig 12). This suggests that mFmn2 can function similar to gFmn2 without inhibiting its activity. Since the gFmn2_tb MO is sequence specific, it would not bind to the mFmn2 and thus mFmn2 will be morpholino resistant. The recue by mFmn2 underscores the evolutional conserved nature of Fmn2 function in these neurons as the

mouse ortholog is able to rescue axon guidance of dI1 commissural neurons in the chick spinal cord

Spinal cords electroporated with Atoh1-gFmn2_N1-GFP or CAG-gFmn2_N1-GFP showed midline crossing defects similar to Fmn2 knock spinal cords. The post-crossing axons that moved longitudinally failed to take the characteristic sharp sigmoid turn and remained closer to the floor plate. We hypothesis that this is due to the dominant negative activity of gFmn2_N1.

gFmn2_N1 electroporated spinals didn't show a significant difference in the axonal tract number ratio as compared to the controls. Since there seems to be a defect in the axonal trajectory, a more qualitative measurement will be ideal for the analysis of phenotypes. One strategy is to measure the angle at which the post-crossing axons extends in the contra-lateral side. Another strategy is to measure the distance to displacement ratio of the post-crossing axons. Both these analysis will provide an insight into the role of Fmn2 in directional motility of dI1 commissural axons.

Formins like mDia, FRL and DAAM has a diaphanous auto-regulatory domain (DAD) C-terminal to the FH2 and a diaphanous inhibitory domain (DID) at the N-teriminus (Higgs, 2005). They are auto-inhibited by the DID-DAD interaction (Fig 2). A Rho GTPase binding domain (GBD) is also present at the N-terminus overlapping the DID. In the case of mDia, binding of Rho GTPase to the GBD is required for escaping the auto-inhibition. But similar regulatory mechanisms are not established in Fmn2. Biochemical studies suggests that Fmn1 N-terminus can interact with its C-terminus and can impair the actin polymerization (Kobielak et al., 2004). Similarly we propose that Fmn2 can be auto-inhibited by the interaction between the C and N terminus. In our experiments the endogenous gFmn2 activity might have got inhibited by the interaction between its C-terminus and the gFmn2_N. Formation of homodimer and FH2-ring is essential for functioning of formins (Campellone and Welch, 2010). gFmn2_N interaction might have inhibited the endogenous gFmn2 from forming the FH2 ring. Hence the phenotypes could be an outcome of the inhibited gFmn2 activity.

4) How does the loss of Fmn2 activity cause midline crossing defect?

The results from our lab suggests a model in which Fmn2 activity is required for the actin polymerization and bundling of actin filaments which in turn is essential for cell adhesion stability. The formation of a stable focal adhesion allows the cell to move in a particular direction.

Supporting the model, we found that inhibiting the Fmn2 in cell lines decreases the focal adhesion area and increases the focal adhesion disassembly rate (Sahasrabudhe, 2015). Knock down studies on primary neuronal cultures showed a decrease in growth cone speed, displacement and directionality (Sahasrabudhe, 2015). Knock down also decreased the filopodia number and length and the growth cone area (Sahasrabudhe, 2015).

If Fmn2 knock down is affecting the focal adhesion maturation and thereby the growth of the axons, we should see a defect in the ipsilateral side of the spinal cord. However we saw an obvious defect only in the post-crossing axons. This suggests that Fmn2 activity is required primarily in the post-crossing axons rather than pre-crossing. It is possible that some guidance cue increases the Fmn2 level or activity in the post-crossing axons.

The non-crossing phenotype we saw in the gFmn2_tb MO treated spinal cord were similar to the neurons misexpressing the truncated Robo1/2 (Reeber et al., 2008). Robo1/2 prevents the post-crossing axons from reentering the Floor plate and drives the post-crossing axons away from the midline. There are evidences showing that RhoGTPases are activated by srGAP upon Robo signaling (Patel and Van Vactor, 2002; Wong et al., 2001). Formins like Dia and DAAM has a GBD and binding of RhoGTPase to the GBD is essential for their activation (Higgs, 2005). Similarly Fmn2 might have a GBD. Robo1/2 might be facilitating the actin nucleation and polymerization in the post-crossing axons via Fmn2, in a Rho dependent manner. Studies on mDia and the Fmn2 results from the lab show that Formins facilitates the directional motility by forming stress fibers and stabilizing the focal adhesions (Faix and Grosse, 2006). Fmn2 knockdown might have inhibited the post-crossing growth by destabilizing the growth cone focal adhesions.

Chapter 5

CONCLUSION

Fmn2 is essential for midline crossing and contra-lateral projection of dI1 commissural neurons. Fmn2 guides the dI1 axons in a cell-autonomous manner. In the dI1 neurons, Fmn2 might be facilitating the growth of post crossing axons by stabilizing the focal adhesions. Since the knockdown is affecting mainly the post-crossing axons, Fmn2 might be active in the axons only after midline crossing. Robo1/2 signaling prevents the post-crossing axons from reentering the Floor plate and drives the axons away from the midlne. The Fmn2 phenotype suggests that the Robo1/2 might be guiding the post-crossing axons by activating the Fmn2 in a Rho dependent manner.

Further experiments are required to identify the signaling between Robo1/2 and Fmn2. Fmn2 levels have to be monitored in the pre and post crossing axons to check for the differential Fmn2 expression upon midline crossing. Studies are required for identifying how the activity of Fmn2 is regulated and whether RhoGTPases plays any role in activating Fmn2. Fmn2-microtubule interaction is another area, which requires further investigation.

Fmn2 defects are associated intellectual disability. Studies on Fmn2 activation and function may lead to discovery of new tools to alleviate the Fmn2 mediated disabilities.

REFERENCE

1. Arakawa, Y., H. Bito, T. Furuyashiki, T. Tsuji, S. Takemoto-Kimura, K. Kimura, K. Nozaki, N. Hashimoto, and S. Narumiya. 2003. Control of axon elongation via an SDF-1alpha/Rho/mDia pathway in cultured cerebellar granule neurons. *J. Cell Biol.* 161:381–91. doi:10.1083/jcb.200210149.
2. Avraham, O., S. Zisman, Y. Hadas, L. Vald, and A. Klar. 2010. Deciphering axonal pathways of genetically defined groups of neurons in the chick neural tube utilizing in ovo electroporation. *J. Vis. Exp.* 6–8. doi:10.3791/1792.
3. Beeraka P. Investigating the role of Arp2/3 and formins in neuronal growth cones. M.S thesis, 2014
4. Campellone, K.G., and M.D. Welch. 2010. A nucleator arms race: cellular control of actin assembly. *Nat. Rev. Mol. Cell Biol.* 11:237–251. doi:10.1038/nrm2867.
5. Chesarone, M. a, A.G. DuPage, and B.L. Goode. 2010. Unleashing formins to remodel the actin and microtubule cytoskeletons. *Nat. Rev. Mol. Cell Biol.* 11:62–74. doi:10.1038/nrm2816.
6. Dent, E.W., S.L. Gupton, and F.B. Gertler. 2011. The growth cone cytoskeleton in Axon outgrowth and guidance. *Cold Spring Harb. Perspect. Biol.* 3:1–39. doi:10.1101/cshperspect.a001800.
7. Eisen, J.S., and J.C. Smith. 2008. Controlling morpholino experiments: don't stop making antisense. *Development*. 135:1735–1743. doi:10.1242/dev.001115.
8. Faix, J., and R. Grosse. 2006. Staying in Shape with Formins. *Dev. Cell*. 10:693–706. doi:10.1016/j.devcel.2006.05.001.
9. Hamburger, V., and H.L. Hamilton. 1951. A series of normal stages in the development of the chick embryo. *J. Morphol.* 88:49–92. doi:10.1002/jmor.1050880104.
10. Higgs, H.N. 2005. Formin proteins: A domain-based approach. *Trends Biochem. Sci.* 30:342–353. doi:10.1016/j.tibs.2005.04.014.
11. Joset, P., A. Wacker, R. Babey, E. a Ingold, I. Andermatt, E.T. Stoeckli, and M. Gesemann. 2011. Rostral growth of commissural axons requires the cell adhesion molecule MDGA2. *Neural Dev.* 6:22. doi:10.1186/1749-8104-6-22.

12. Kaprielian, Z., R. Imondi, and E. Runko. 2000. Axon Guidance at the Midline of the Developing CNS. 176–197.
13. Kobielak, A., H.A. Pasolli, and E. Fuchs. 2004. Mammalian formin-1 participates in adherens junctions and polymerization of linear actin cables. *Nat. Cell Biol.* 6:21–30. doi:10.1038/ncb1075.
14. Korobova, F., and T. Svitkina. 2008. Arp2/3 complex is important for filopodia formation, growth cone motility, and neuritogenesis in neuronal cells. *Mol. Biol. Cell*. 19:1561–74. doi:10.1091/mbc.E07-09-0964.
15. Kos, R., R.P. Tucker, R. Hall, T.D. Duong, and C. a. Erickson. 2003. Methods for introducing morpholinos into the chicken embryo. *Dev. Dyn.* 226:470–477. doi:10.1002/dvdy.10254.
16. Krull, C.E. 2004. A Primer on Using in Ovo Electroporation to Analyze Gene Function. *Dev. Dyn.* 229:433–439. doi:10.1002/dvdy.10473.
17. Leader, B., and P. Leder. 2000. Formin-2, a novel formin homology protein of the cappuccino subfamily, is highly expressed in the developing and adult central nervous system. *Mech. Dev.* 93:221–231. doi:10.1016/S0925-4773(00)00276-8.
18. Li, F., and H.N. Higgs. 2003. The Mouse Formin mDia1 Is a Potent Actin Nucleation Factor Regulated by Autoinhibition. *Curr. Biol.* 13:1335–1340. doi:10.1016/S0960-9822(03)00540-2.
19. Lowery, L.A., and D. Van Vactor. 2009. The trip of the tip: understanding the growth cone machinery. *Nat. Rev. Mol. Cell Biol.* 10:332–43. doi:10.1038/nrm2679.
20. Lu, J., W. Meng, F. Poy, S. Maiti, B.L. Goode, and M.J. Eck. 2007. Structure of the FH2 domain of Daam1: implications for formin regulation of actin assembly. *J. Mol. Biol.* 369:1258–69. doi:10.1016/j.jmb.2007.04.002.
21. Muramatsu, T., Y. Mizutani, Y. Ohmori, and J. Okumura. 1997. Comparison of three nonviral transfection methods for foreign gene expression in early chicken embryos in ovo. *Biochem. Biophys. Res. Commun.* 230:376–380. doi:10.1006/bbrc.1996.5882.
22. Nakamura, H., T. Katahira, T. Sato, Y. Watanabe, and J.I. Funahashi. 2004. Gain- and loss-of-function in chick embryos by electroporation. *Mech. Dev.* 121:1137–1143. doi:10.1016/j.mod.2004.05.013.

23. Patel, B.N., and D.L. Van Vactor. 2002. Axon guidance: The cytoplasmic tail. *Curr. Opin. Cell Biol.* 14:221–229. doi:10.1016/S0955-0674(02)00308-3.
24. Pring, M., M. Evangelista, C. Boone, C. Yang, and S.H. Zigmond. 2003. Mechanism of formin-induced nucleation of actin filaments. *Biochemistry*. 42:486–96. doi:10.1021/bi026520j.
25. Pruyne, D., M. Evangelista, C. Yang, E. Bi, S. Zigmond, A. Bretscher, and C. Boone. 2002. Role of formins in actin assembly: nucleation and barbed-end association. *Science*. 297:612–5. doi:10.1126/science.1072309.
26. Reeber, S.L., N. Sakai, Y. Nakada, J. Dumas, K. Dobrenis, J.E. Johnson, and Z. Kaprielian. 2008. Manipulating Robo expression in vivo perturbs commissural axon pathfinding in the chick spinal cord. *J. Neurosci.* 28:8698–8708. doi:10.1523/JNEUROSCI.1479-08.2008.
27. Sahasrabudhe A. Formin-2 in growth cone motility and guidance. Phd thesis, 2015 (submitted, defence awaited)
28. Sakai, N., R. Insolera, R. V. Sillitoe, S.-H. Shi, and Z. Kaprielian. 2012. Axon Sorting within the Spinal Cord Marginal Zone via Robo-Mediated Inhibition of N-Cadherin Controls Spinocerebellar Tract Formation. *J. Neurosci.* 32:15377–15387. doi:10.1523/JNEUROSCI.2225-12.2012.
29. San Miguel-Ruiz, J.E., and P.C. Letourneau. 2014. The Role of Arp2/3 in Growth Cone Actin Dynamics and Guidance Is Substrate Dependent. *J. Neurosci.* 34:5895–5908. doi:10.1523/JNEUROSCI.0672-14.2014.
30. Schumacher, N., J.M. Borawski, C.B. Leberfinger, M. Gessler, and E. Kerkhoff. 2004. Overlapping expression pattern of the actin organizers Spir-1 and formin-2 in the developing mouse nervous system and the adult brain. *Gene Expr. Patterns*. 4:249–255. doi:10.1016/j.modgep.2003.11.006.
31. Stoeckli, E.T., and L.T. Landmesser. 1995. Axonin-1, Nr-CAM, and Ng-CAM play different roles in the in vivo guidance of chick commissural neurons. *Neuron*. 14:1165–1179. doi:10.1016/0896-6273(95)90264-3.
32. Vizcarra, C.L., B. Kreutz, A. a Rodal, A. V Toms, J. Lu, W. Zheng, M.E. Quinlan, and M.J. Eck. 2011. Structure and function of the interacting domains of Spire and

Fmn-family formins. *Proc. Natl. Acad. Sci. U. S. A.* 108:11884–11889. doi:10.1073/pnas.1105703108.

33. Wong, K., X.R. Ren, Y.Z. Huang, Y. Xie, G. Liu, H. Saito, H. Tang, L. Wen, S.M. Brady-Kalnay, L. Mei, J.Y. Wu, W.C. Xiong, and Y. Rao. 2001. Signal transduction in neuronal migration: Roles of GTPase activating proteins and the small GTPase Cdc42 in the Slit-Robo pathway. *Cell*. 107:209–221. doi:10.1016/S0092-8674(01)00530-X.
34. Xu, Y., J.B. Moseley, I. Sagot, F. Poy, D. Pellman, B.L. Goode, and M.J. Eck. 2004. Crystal structures of a formin homology-2 domain reveal a tethered dimer architecture. *Cell*. 116:711–723. doi:10.1016/S0092-8674(04)00210-7.
35. Zisman, S., K. Marom, O. Avraham, L. Rinsky-Halivni, U. Gai, G. Kligun, V. Tzarfaty-Majar, T. Suzuki, and A. Klar. 2007. Proteolysis and membrane capture of F-spondin generates combinatorial guidance cues from a single molecule. *J. Cell Biol.* 178:1237–1249. doi:10.1083/jcb.200702184.